SLAC-PUB-1406
(A)
April 1974

ACTIVATION OF ALUMINUM BEAM DUMPS BY HIGH-ENERGY ELECTRONS AT SLAC*

William P. Swanson
Stanford Linear Accelerator Center
Stanford University, Stanford, Calif. 94305

ABSTRACT

Water-cooled Al beam dumps are used at SLAC to absorb the energy of high-intensity electron beams through development of a massive electromagnetic cascade. The aluminum becomes activated and constitutes a moderate radiation hazard. Decay-curve measurements made near two such dump installations are presented and compared with calculation. The most important radionuclides produced in the Al are identified as $^{24}Na(T_{\frac{1}{2}} = 14.96\ h)$ and $^{22}Na(T_{\frac{1}{2}} = 2.62\ yr)$. It is found that other activated materials, particularly Fe shielding, can increase the exposure rates near such installations significantly, and must be considered. A formula is given which is useful for predicting dose rates for operational health-physics use. Recommendations are made with a view to reducing doses to personnel who must work in the vicinity of such installations.

(Submitted to Health Physics)

---

* Work supported by the U.S. Atomic Energy Commission.

Paper presented at the 18th Annual Meeting of the Health Physics Society, Miami Beach, June 17-21, 1973.

I. Introduction

In order to make possible experiments using a wide variety of particle types at the Stanford Linear Accelerator Center, the primary electron beam is divided into several different beam channels. Each of these primary electron beams then may be made to strike a target and give rise to secondary particles which are transported to the experimental area. The unused power of the electron beam is absorbed in some sort of power-absorbing device called the beam dump. These beam dumps may vary greatly in their geometry and material (Kilert et al., 1968) but a typical construction is a water-cooled aluminum arrangement designed to absorb average beam powers in the range of 50 kW to 250 kW. They are devices essential to the safe operation of the accelerator because the beam power they absorb could otherwise burn through uncooled shielding material placed in the beam path.

During accelerator operation, lethal exposure rates are produced by the electron beam impinging on these beam dumps and they are therefore heavily shielded and no access is permitted. During the accelerator "down times", occasional work must be done in their vicinity, including repair or removal. The beam dump itself becomes radioactive through use as does the surrounding shielding material. Together,they therefore constitute a moderate radiation hazard which must be controlled by responsible health physicists. This paper describes calculations to evaluate the extent of this hazard. Measurements of exposure rates are made near two such installations and compared with calculations. Finally, we give recommendations for the proper handling and shielding of these electron beam dumps.

Figure 1 shows the construction of D-62, a dump rated at 135 kW. It is basically a stack of 119 plates of 3/4" aluminum separated by 1/4" voids where

water circulates. Figure 2 shows the construction of D-30, a dump rated at 250 kW. It is more complicated, consisting of several stages of different types of materials. However, the ten-radiation-length portion where most of the beam power is dissipated is again a combination of aluminum and water (65% and 35% respectively, by volume). D-62 comprises a total of 25 radiation lengths, and D-30 a total of 40 radiation lengths of material. Both are therefore long enough to absorb virtually all the power of the electron beam. However they are both narrow enough that a non-negligible fraction of the beam power escapes to the side, mainly in the form of electromagnetic radiation and neutrons. This fraction is hard to estimate but it must be of the order of a few percent. This leakage radiation requires the area about the dump to be on "no access" status during accelerator operation and may activate iron shielding or other material in the vicinity during operation. A separate study of activation induced in Fe shielding is given by Swanson (1974a).

II. Calculation

In the electromagnetic cascade which occurs in the dump, large numbers of secondary electrons, positrons, and photons are present. It is mainly the photons in the shower which induce spallation reactions leading to residual activity. Spallation products which could be of importance are shown in Table 1. We include only gamma and β^+ — emitters having half-lives greater than a few minutes, and rank them in order of decreasing mass number (Lederer, et al., 1967). Therefore, those higher in the table are closer in mass number to the target ^{27}Al and involve the emission of fewer secondary particles. The nuclides $^{26}Al^{m}$($T_{\frac{1}{2}} = 6.37$ s) and ^{26}Al($T_{\frac{1}{2}} = 7.4 \cdot 10^5$ y), which are easily produced by the (γ,n) reaction, are omitted because of excessively short and long half-lives, as are several others because of short half-life.

Information on these spallation cross sections is rather sketchy. The cross sections used are given in Table 1 in a form integrated over all photon energies E_γ weighted by the inverse energy squared:

$$\sigma_{-2} \equiv \int_0^{E_0} \frac{\sigma(E_\gamma)}{E_\gamma^2} \, dE_\gamma \, . \qquad (1)$$

This is a convenient formulation to use in these calculations because the photon track-length distribution in an electromagnetic cascade behaves approximately as inverse energy squared (Rossi, 1952):

$$\frac{dL}{dE_\gamma} = 0.572 \, \frac{E_0 X_0}{E_\gamma^2} \, , \qquad (2)$$

where E_0 is the incident electron energy, and the dimensions of the track length L are given by the radiation length X_0.

The values of σ_{-2} in Table 1 were obtained from various sources. For ^{24}Na, a numerical integration was performed, using the data of Meyer et al. (1968), for the threshold region ($E_\gamma \sim 31$ - 175 MeV), of Masaike (1964) for the region E_γ = 175 - 725 MeV, of di Napoli et al. (1971a), for E_γ = 725 - 1000 MeV, of Andersson et al. (1972), for E_γ = 1 - 7 GeV, and of Jenkins and Warren (1973) for E_γ to 19 GeV. Experiments are in poor agreement in the important lower-energy range. Gorbunov et al. (1960) report cross sections about 40% smaller than those of Meyer et al. and those of Saito (1971) are about 2-3 times larger. Thus the value of σ_{-2} for ^{24}Na could be uncertain by this amount.

Data are more sketchy for the other spallation products, and completely lacking in the near-threshold region. However, for all nuclides considered there are available data on high-energy spallation yields (di Napoli et al. 1971a; Jenkins and Warren, 1973; Kumbartzki et al., 1971; Fulmer et al. 1970; Callis, 1968; di Napoli et al., 1971b; di Napoli et al., 1973a; di Napoli et al., 1973b). The value of σ_{-2} found for ^{24}Na as described above was then scaled by the ratio of the spallation yield of the nuclide in question to the yield for ^{24}Na found in the same experiment. Where more than one experiment was available, the lower-energy one was chosen. This procedure is satisfactory if the yields for the nuclide in question and for ^{24}Na have the same relative energy dependence. Apart from obvious differences in threshold energies,* this would be consistent with the cascade-evaporation hypothesis (Kumbartzki et al., 1971; Jonsson and Lindgren, 1973). The rationale and method of this procedure are presented in greater detail elsewhere (Swanson, 1974b).

Values of the specific gamma-ray constant Γ were obtained from standard tables (Radiological Health Handbook, 1970), and, assuming an unshielded point source, saturation exposure rates were calculated from the formula (DeStaebler, 1963; Barbier, 1969)

$$\dot{X}_s = \left[\frac{P}{e E_0}\right] \cdot \left[\frac{N_0}{A}\right] \cdot \left[0.572\, E_0\, X_0\, \sigma_{-2}\right] \cdot \left[\frac{\Gamma}{3.7 \cdot 10^{10}}\right], \quad (3)$$

* Note that in measuring a yield from a thin-target bremsstrahlung beam, the experiment is essentially measuring an average cross section, weighted by approximately E_γ^{-1}. This is different from the desired weighting (Eq. 1). Because of weighting, the threshold region is emphasized, and differing threshold energies could be expected to cause significant deviations from the simple scaling used. The method is nevertheless used, for lack of better information.

in which the first factor converts the average beam power P to electrons per second, using the electronic charge e and energy E_0. The third factor is motivated by the discussion above. The remaining factors are self-explanatory. After cancelling out E_0 and combining constant factors, we have for the saturation exposure rate

$$\dot{X}_s(\mathrm{R\,h^{-1}\,m^2}) = 5.81\ 10^{-2}\ \mathrm{P(kW)}\ \frac{X_0(\mathrm{gm\ cm^{-2}})}{A(\mathrm{gm})}\ \sigma_{-2}(\mu\mathrm{b\ MeV^{-1}})\ \Gamma(\mathrm{R\,h^{-1}\,m^2\,Ci^{-1}}). \quad (4)$$

For Al, we use $X_0 = 23.88$ gm cm^{-2} for the radiation length (Knasel, 1970), and $A = 26.98$ gm.

We simplify these calculations by assuming that the equations for an unshielded point source are adequate for the accuracy of this comparison. The activity is actually distributed along the electron beam line, peaking at 2-3 X_0, and decreasing to half intensity at about 1 X_0 and 5 X_0 (Fulmer et al., 1969). This is qualitatively shown by contact exposure rates plotted in Figs. 1 and 2 which peak in this region but have a broader distribution than the activity distribution.

It is evident from these calculations (Table 1) that the two isotopes ^{24}Na and ^{22}Na dominate, giving rise to saturation exposure rates of 51 R h^{-1} m^2 and 30 R h^{-1} m^2, respectively, for 100 kW continuous power. This is illustrated in Fig. 3 which shows contributions to the exposure rate of each of these radionuclides as a function of decay time. It is seen that ^{24}Na, with a 14.96-hour half-life, dominates over all shorter-lived spallation products. ^{22}Na will also be important, but its contribution has not been added into the total exposure rate in Fig. 3 because saturation is not generally reached over the useful lifetime of the beam dumps at SLAC. Thus, a special calculation is needed to estimate its contribution in each particular case. However, it is clear that after some time,

generally a few days, ^{22}Na will be the only remaining significant contributor to the total exposure rate. Its presence may cause the beam dump to be a radiation hazard for several years.

We emphasize that the σ_{-2}, and consequently the $\dot{X}_s$ of Table 1 could be uncertain by as much as a factor of two. For this reason corrections for self-shielding and for the true distribution of activity were not made. Nevertheless, the relative importance of these nuclides is clearly shown by Table 1 and Fig. 3, and useful estimates of exposure rates can be made from these data.

Photospallation reactions on the oxygen in the cooling water (Warren et al., 1969) can also lead to the production of such radionuclides as ^{15}O, ^{13}N, ^{11}C and ^{7}Be. These radionuclides are much less of a problem owing to the fact that water constitutes a small fraction of the dump, as measured in radiation lengths (8% for D-62, 12% for D-30). Concentrations are also reduced by dilution in the total volume of the cooling system through which the water circulates and by the relatively short half-lives involved. ^{7}Be, which has a 53.3-day half-life, is filtered out of the water by an ion-exchange process having a removal half-life of about 10 hours. Therefore, we neglect the contribution of the water to exposure rates near the Al dumps.

III. Measurement

Measurements on exposure rates as a function of decay time were made in the vicinity of these dump-installations, starting within an hour of accelerator shutoff. An Argon-filled ionization chamber was placed near each of these dumps and its readings were recorded on a chart recorder over a period of days, after which only daily measurements were made. The actual beam power just before turnoff was about 100 kW on both dumps.

Figures 4 and 5 show the exposure rate measured at D-62 and the rate calculated as just described. It can be seen that the prediction is qualitatively correct in that the ^{24}Na 14.96-hour activity dominates for about five days, after which ^{22}Na activity dominates. Deviations from this simple picture are evident which we attribute to other materials; In the case of D-62, a $\frac{1}{4}$"-thick stainless steel secondary-emission monitor directly in the beam path (Fig. 1) probably explains the short-lived (3-4 h) activity (Fig. 4) and perhaps the deviation at about 5-8 days (Fig. 5). The prediction for ^{24}Na is about a factor of 1.5 greater than the measurement. This amount of discrepancy is within the assumed accuracy of the calculation.

We take the decay curve of D-30 as an example of a more complicated situation which is encountered. As Fig. 2 shows, D-30 is constructed of materials in addition to aluminum, the main energy-absorbing material. Moreover, D-30 was surrounded by shielding material packed very close in. Exposure rate measurements were made by removing a few iron bricks from the shield in order to insert the ionization chamber. Therefore these measurements were made at 1 foot rather than 1 meter. Figure 6 shows the decay curve thus measured. As expected, the two isotopes of Na both play an important role. The exposure rate due to ^{24}Na is overestimated by the calculation, but is within the expected uncertainty. It was found that the iron in the shield had become activated and its contribution to the exposure rate measured was comparable to that of the ^{22}Na over the period shown in Fig. 6. A special study made of the activity induced in the iron is presented separately (Swanson, 1974a). The exposure rate at D-30 was measured a year later when the dump had been removed and stood clear of its shielding material. That measurement was consistent with the hypothesis that only ^{22}Na contributed substantially at that time.

IV. Conclusion and Recommendations

From this study we have identified the principal radionuclides and gathered sufficient information on their production to predict exposure rates from aluminum-dump installations with sufficient accuracy for most operational radiation-protection purposes (i.e., to within a factor of 1.5). The exposure rates near an unshielded aluminum dump at any time t may be estimated by combining two terms of the form

$$\dot{X} = \dot{X}_s \left\{ \frac{\ell n\, 2}{T_{\frac{1}{2}}} \int_{-\infty}^{0} P(t') \exp\left(\frac{t'\, \ell n\, 2}{T_{\frac{1}{2}}}\right) dt' \right\} \exp\left(\frac{-t\, \ell n\, 2}{T_{\frac{1}{2}}}\right), \qquad (5)$$

to account for the Na nuclides. We use $\dot{X}_s$, the saturation dose rate per unit power (Table 1). The term in brackets is an integral of the power as a function of time P(t') over the life of the dump, which describes activity buildup until the time of most recent beam shutoff t = 0. The last factor describes exponential decay following shutoff.

At SLAC the useful lifetime of a dump is typically less than $T_{\frac{1}{2}}(^{22}Na)$=2.62 yr, and periods of operation and downtime are typically 4-8 weeks, which is long compared to $T_{\frac{1}{2}}(^{24}Na)$ = 14.96 h. Thus, for rapid calculation, we use the approximation derived from Eq. (5), using rounded input data from Table 1:

$$\dot{X}(R\,h^{-1}\,m^2) = 0.5\, P_{recent}(kW) \cdot \exp(-t(h)(\ell n\, 2)/15) + 2 \cdot 10^{-4}\, \Sigma[P(kW) \cdot T(days)] \qquad (6)$$

where the first term uses P_{recent}, the average power level during the few days preceding shutoff, to account for ^{24}Na buildup, and considers the 15-hour decay that follows. The second term uses an estimate based on kilowatt-days, summed over running periods, to describe buildup of ^{22}Na, and then ignores decay over the remaining dump lifetime. This is a convenient formulation to estimate exposure rates during the few-week periods of shutdown, because it uses input in a

form easily obtainable from operations logbooks. Measurements indicate that Eq. (6) will provide a conservative estimate for most of the period of several days when exposure rates are greatest due to ^{24}Na. Since we found that shielding and other materials may contribute substantially, these effects must be considered in each particular case and added to Eq. (5) or (6) as necessary.

On the basis of this experience, we have made a number of recommendations to the SLAC Experimental Facilities Department (EFD) along these lines:

1. Work in the vicinity of these dumps is postponed by about one week from the time of beam shut off in order to allow the 15-hour ^{24}Na activity to decay.

2. The most serious doses to individuals have been imparted during the removal of one of these dumps, D-30. Therefore several suggestions were made to reduce the time required to disconnect and rig the dump.

3. In view of our finding that the dismantling and handling of shielding nearest D-30 contributed to doses, we proposed the substitution of lead or concrete for iron, and rationalization of the shield design for easier handling.

Acknowledgments

I am grateful to Dr. Richard C. McCall for suggesting this study and helping to set up the initial measurements, and to my colleagues in the Health Physics Group and Experimental Facilities Department at SLAC for useful background information.

REFERENCES

Andersson, G., Blomqvist, I., Forkman, B., Jonsson, G.G., Järund, A., Kroon, I., Lindgren, K., Schrøder, B., and Tesch, K., 1972, Nucl. Phys. A197, 44.

Barbier, M., 1969, Induced Radioactivity, Chap. V (North-Holland Publishing Company, Amsterdam-London).

Callis, E.L., 1968, "Electrodisintegration of Aluminum, Iron, Nickel, and Copper at 13.3 and 16 GeV," Oak Ridge National Laboratory Report No. ORNL-TM-2309.

DeStaebler, H., 1963, "Photon-Induced Residual Activity," Stanford Linear Accelerator Center, Report No. TN-63-92.

di Napoli, V., Lacerenza, A.M., Salvetti, F., de Carvalho, H.G., and Martins, J.B., 1971a, Lettere al Nuovo Cimento 1, 835.

di Napoli, V., Margadonna, D., Salvetti, F., de Carvalho, H.G., and Martins, J.B., 1971b, Nucl. Instr. and Meth. 93, 77.

di Napoli, V., Lacerenza, A.M., Salvetti, F., Terenzi, S.M., de Carvalho, H.G., and Martins, J.B., 1973a, J. Inorg. Nucl. Chem. 35, 1419.

di Napoli, V., Salvetti, F., Terranova, M.L., de Carvalho, H.G., and Martins, J.B., 1973b, "Photon-Induced Fragmentation in ^{27}Al and ^{32}S by 1-GeV Bremsstrahlung," Rome-Rio de Janeiro collaboration, Preprint.

Fulmer, C.B., Williams, I.R., Toth, K.S., and Dell, G.F., 1969, Phys. Rev. 188, 1752.

Fulmer, C.B., Toth, K.S., Williams, I.R., Handley, T.H., Dell, G.F., Callis, E.L., Jenkins, T.M., and Wyckoff, J.M., 1970, Phys. Rev. C2, 1371.

Gorbunov, A.N., Denisov, F.P., and Kolotukhin, V.A., 1960, Soviet Phys.-JETP 11, 783.

Jenkins, T.M., and Warren, G.J., 1973, Stanford Linear Accelerator Center, private communication.

Jonsson, G.G., and Lindgren, K., 1973, Physica Scripta 7, 49.

Kilert, A.H., Lucas, L.R., Scott, W.S., and Walz, D.R., Ed., 1968, "Beam Power Absorption Devices," in "The Stanford Two-Mile Accelerator," R.B. Neal, Gen. Ed. (Benjamin, New York) pp. 705-774.

Knasel, T.M., 1970, Nucl. Instr. and Meth. 83, 217.

Kumbartzki, G.J., Kim, U., and Kwan, Ch. K., 1971, Nucl. Phys. A160, 237.

Lederer, C.M., Hollander, J.M., and Perlman, I., 1967, "Table of Isotopes," Sixth Ed., (Wiley, New York).

Masaike, A., 1964, J. Phys. Soc. Japan 19, 427.

Meyer, R.A., Walters, W.B., and Hummel, J.P., 1968, Nucl. Phys. A122, 606.

Radiological Health Handbook, 1970, U.S. Dept. of Health, Education and Welfare, Public Health Service (Washington), pp. 131-132.

Rossi, Bruno, 1952, "High Energy Particles," (Prentice Hall, Inc., Inglewood Cliffs, N.J.) p. 271.

Saito, T., 1971, Bull. Chem. Soc. Japan 44, 1800.

Swanson, W.P., 1974a, "Activation of Iron Shielding Near High-Energy Electron Beam Dumps," Stanford Linear Accelerator Center, in preparation.

Swanson, W.P., 1974b, "Predictions of Photo-Induced Activity in Aluminum," Stanford Linear Accelerator Center, Technical Note, in preparation.

Warren, G.J., Busick, D.D., and McCall, R.C., 1969, "Radioactivity Produced and Released from Water at High-Energies," in Second Intl. Conference on Accelerator Dosimetry and Experience, U.S. Atomic Energy Commission Report No. CONF-6911-01, p. 99.

TABLE 1

PHOTOSPALLATION PRODUCTS IN ^{27}Al

Spallation Product	Half-Life	σ_{-2} (μb/MeV)	Γ Specific Gamma-Ray Constant ($R\ h^{-1}\ m^2\ Ci^{-1}$)	$\dot{X}_s$ Saturation Exposure Rate (100 kW) ($R\ h^{-1}\ m^2$)
^{24}Na	14.96 h	5.4	1.84	51
^{24}Ne	3.38 min	0.07	0.32	0.1
^{22}Na	2.62 yr	4.7	1.20	30
^{18}F	109.7 min	2.8	0.58	8
^{15}O	123 sec	1.4	0.6	4
^{13}N	9.96 min	0.3	0.6	0.8
^{11}C	20.34 min	1.0	0.59	3.0
^{7}Be	53.6 days	2.3	0.03	0.4

FIGURE CAPTIONS

1. The construction of dump D-62, composed of 3/4" plates of aluminum separated by 1/4" gaps of water. Two vacuum pipes extend through the length of the dump and protrude at the right, to transport secondary beams from a target just upstream. The primary electron-beam energy is mostly absorbed in the first portion of the dump. The upper portion of the figure shows the scale as measured in radiation lengths. Plotted points are contact exposure rates to indicate the approximate distribution of induced activity.
2. The construction of dump D-30. The primary electron beam passes through about one radiation-length of beryllium, followed by one radiation-length of stainless-steel tubing wall, and then enters the main portion of the dump which is filled with aluminum spheres, cooled by water. The electron beam is finally absorbed at the end of the dump in a block of solid copper. Secondary muon beams from an upstream target are transported through a beryllium filter and pion beams through a vacuum pipe. The upper portion of the figure shows the scale as measured in radiation lengths. Plotted points are contact exposure rates which indicate the approximate distribution of induced activity. These were measured after the dump had been removed from its shield.
3. Predicted saturation exposure rates at 1 meter for an aluminum dump absorbing 100 kW continuously. The contributions of ^{22}Na and ^{7}Be have not been added to the total because in practice saturation is not achieved for these nuclides.
4. Exposure rate measured at one meter from dump D-62 as a function of decay time. The solid line is the contribution of ^{24}Na inferred from these data, and the dashed line is the prediction described in the text.

5. Measured exposure rate at one meter from dump D-62 as in Fig. 4 but with expanded time scale. Curves are predictions described in the text.

6. Measured exposure rate at one foot from dump D-30 as a function of decay time. Curves are predictions described in the text. D-30 was enclosed in shielding material which became activated and contributed significantly to the measured exposure rate.

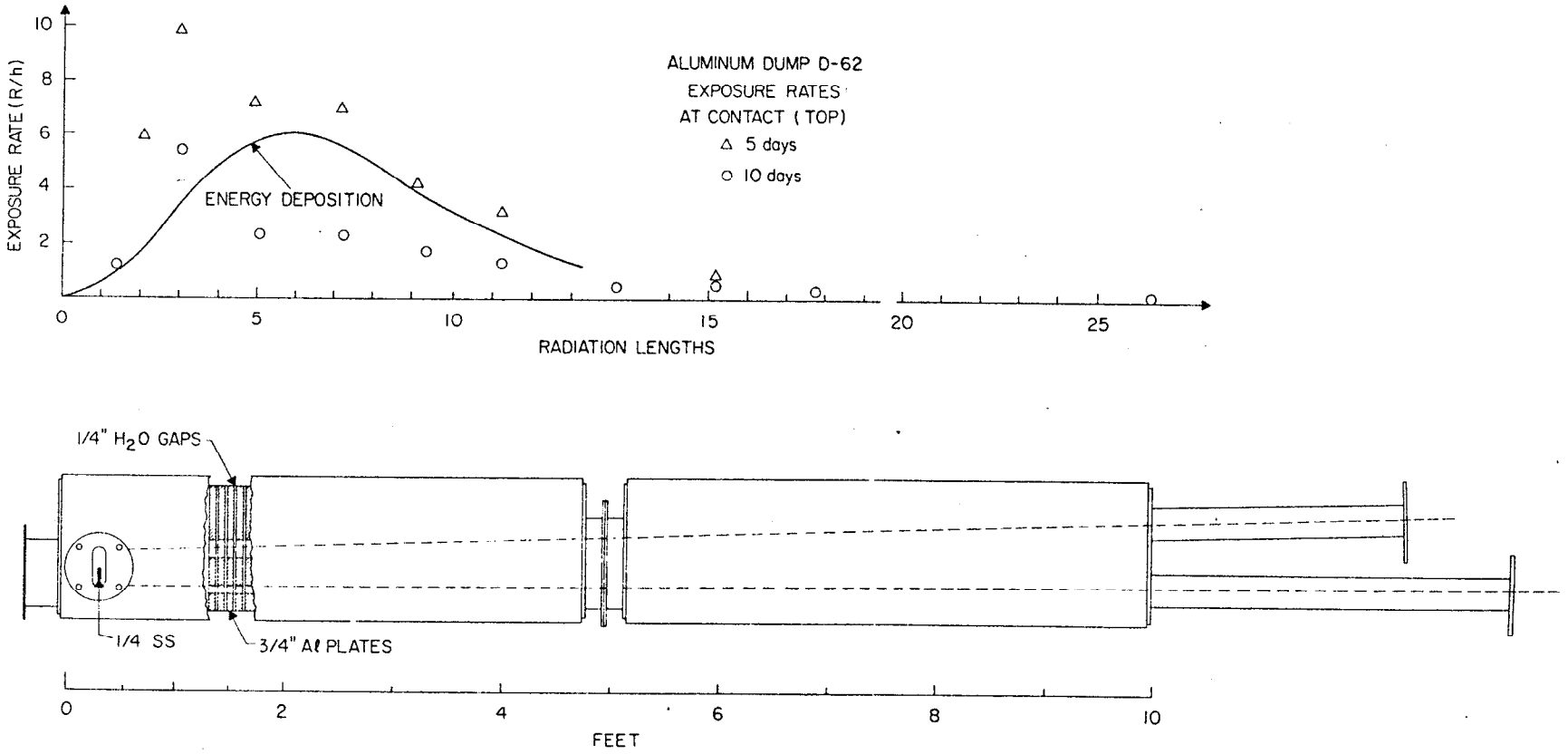
EXPOSURE RATE (R/h)
10
8
6
4
2
0
5
10
15
20
25
RADIATION LENGTHS
ENERGY DEPOSITION
ALUMINUM DUMP D-62
EXPOSURE RATES
AT CONTACT (TOP)
△ 5 days
○ 10 days
1/4" H_2O GAPS
1/4 SS
3/4" Al PLATES
0
2
4
6
8
10
FEET

Fig. 1

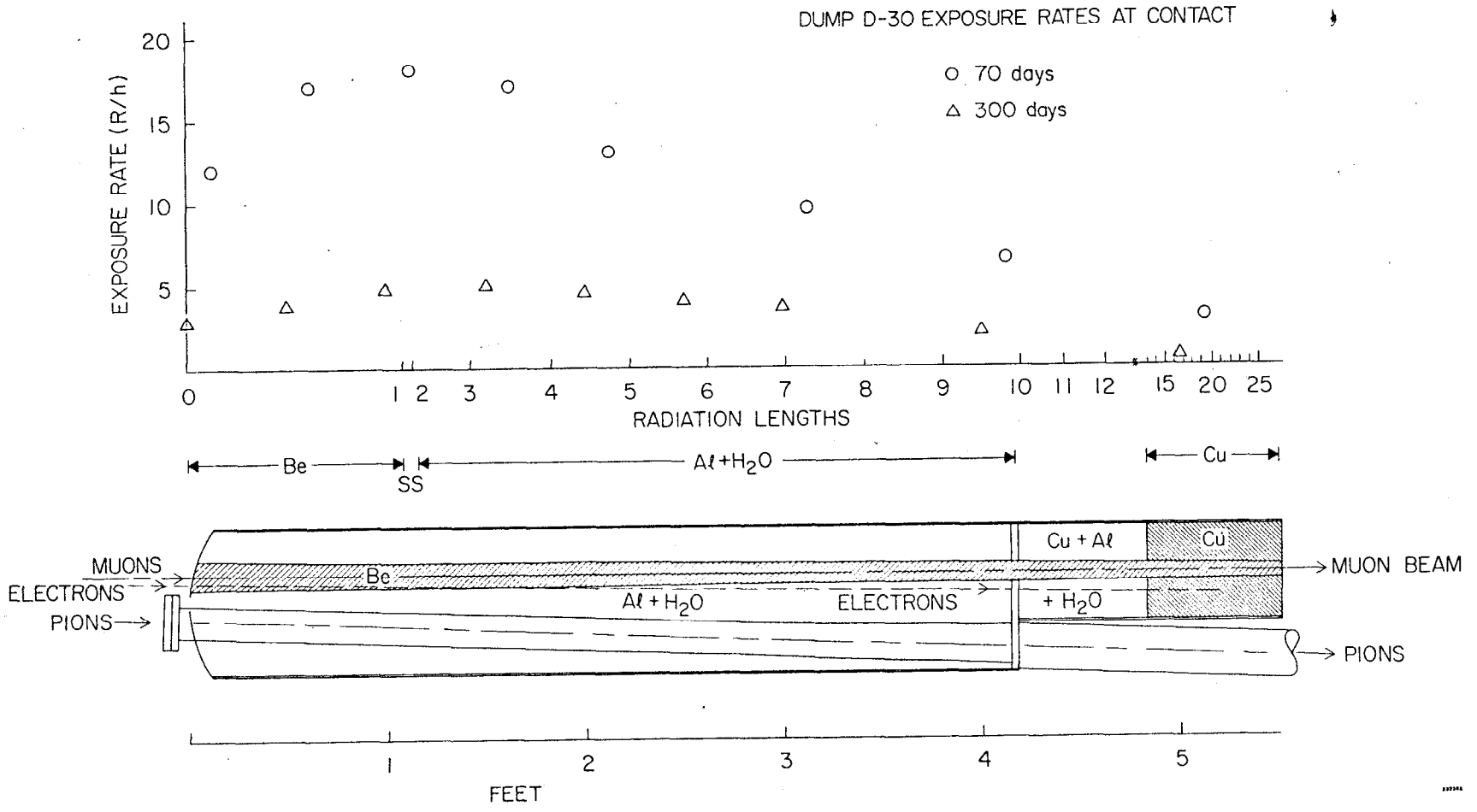
DUMP D-30 EXPOSURE RATES AT CONTACT
70 days
300 days
EXPOSURE RATE (R/h)
20
15
10
5
0
1 2 3 4 5 6 7 8 9 10 11 12 15 20 25
RADIATION LENGTHS
Be
SS
Al+H2O
Cu
MUONS
ELECTRONS
PIONS
Be
Al + H2O
ELECTRONS
Cu + Al
+ H2O
Cu
MUON BEAM
PIONS
1 2 3 4 5
FEET

Fig. 2

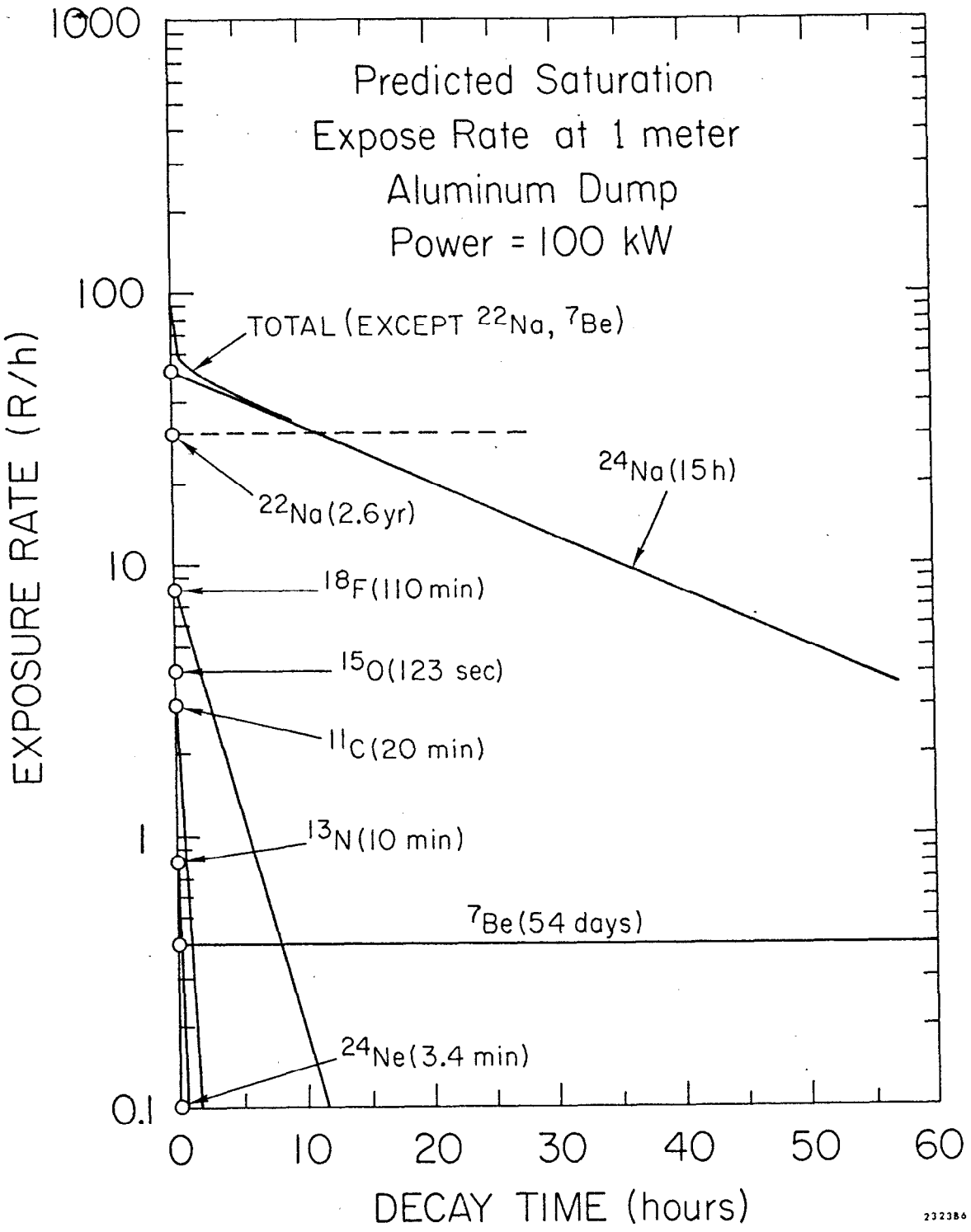
Predicted Saturation
Expose Rate at 1 meter
Aluminum Dump
Power = 100 kW
TOTAL (EXCEPT 22Na, 7Be)
24Na(15h)
22Na(2.6yr)
18F(110 min)
15O(123 sec)
11C(20 min)
13N(10 min)
7Be(54 days)
24Ne(3.4 min)
EXPOSURE RATE (R/h)
1000
100
10
1
0.1
0
10
20
30
40
50
60
DECAY TIME (hours)
232386

Fig. 3

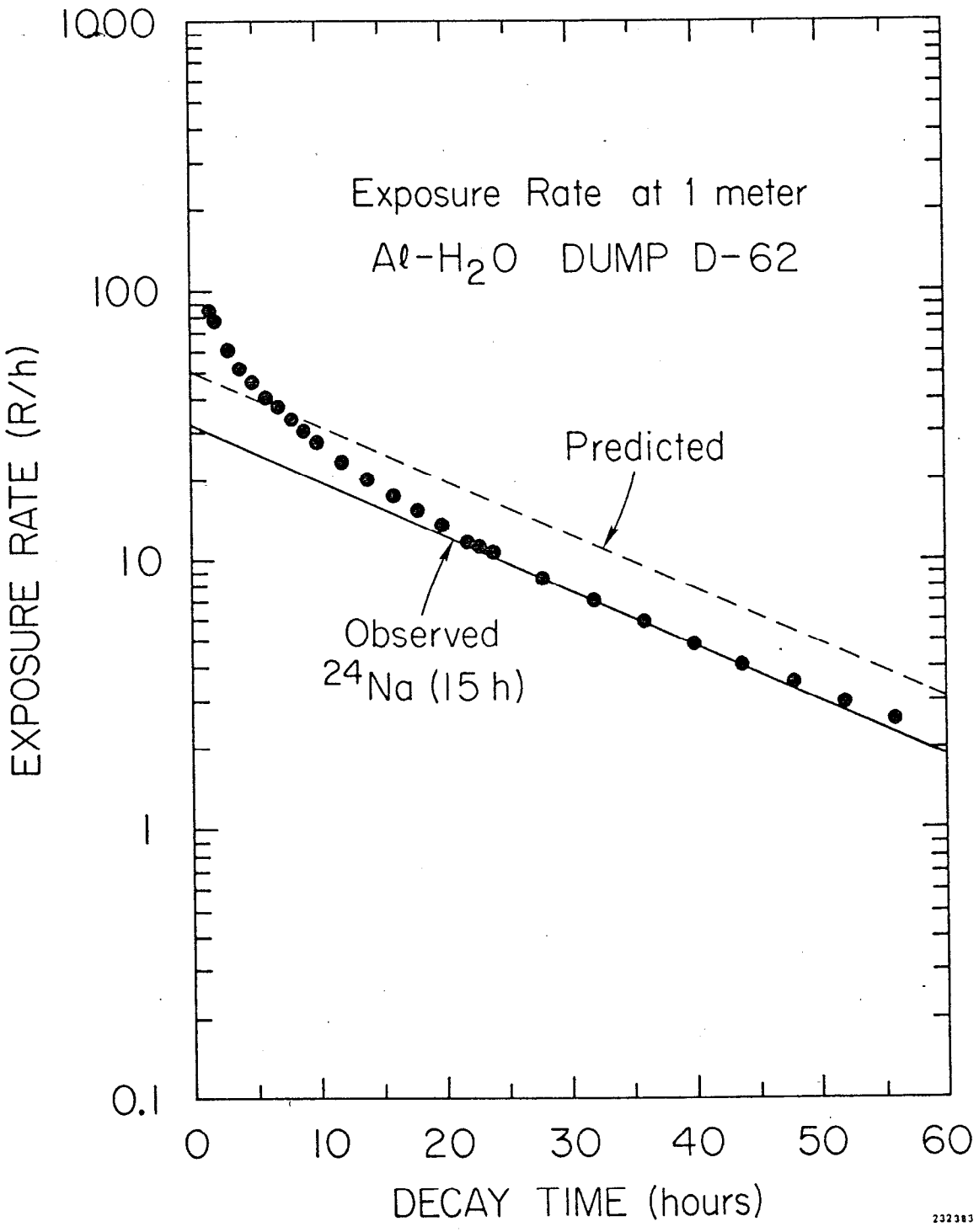
1000
100
10
1
0.1
EXPOSURE RATE (R/h)
Exposure Rate at 1 meter
Aℓ-H2O DUMP D-62
Predicted
Observed
24Na (15 h)
0
10
20
30
40
50
60
DECAY TIME (hours)
232383

Fig. 4

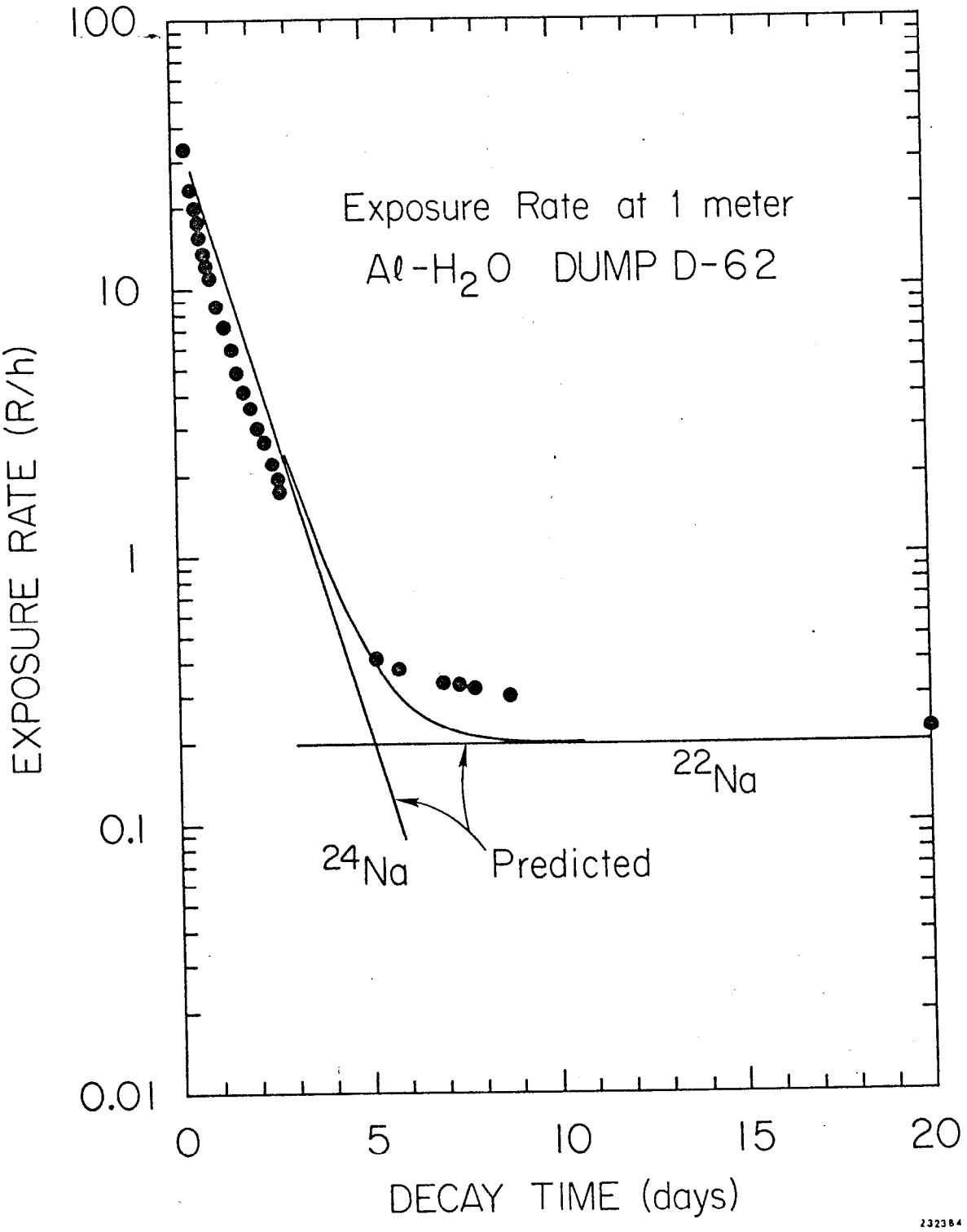
Exposure Rate at 1 meter
Al-H2O DUMP D-62
EXPOSURE RATE (R/h)
100
10
1
0.1
0.01
0
5
10
15
20
DECAY TIME (days)
22Na
24Na
Predicted
232384

Fig. 5

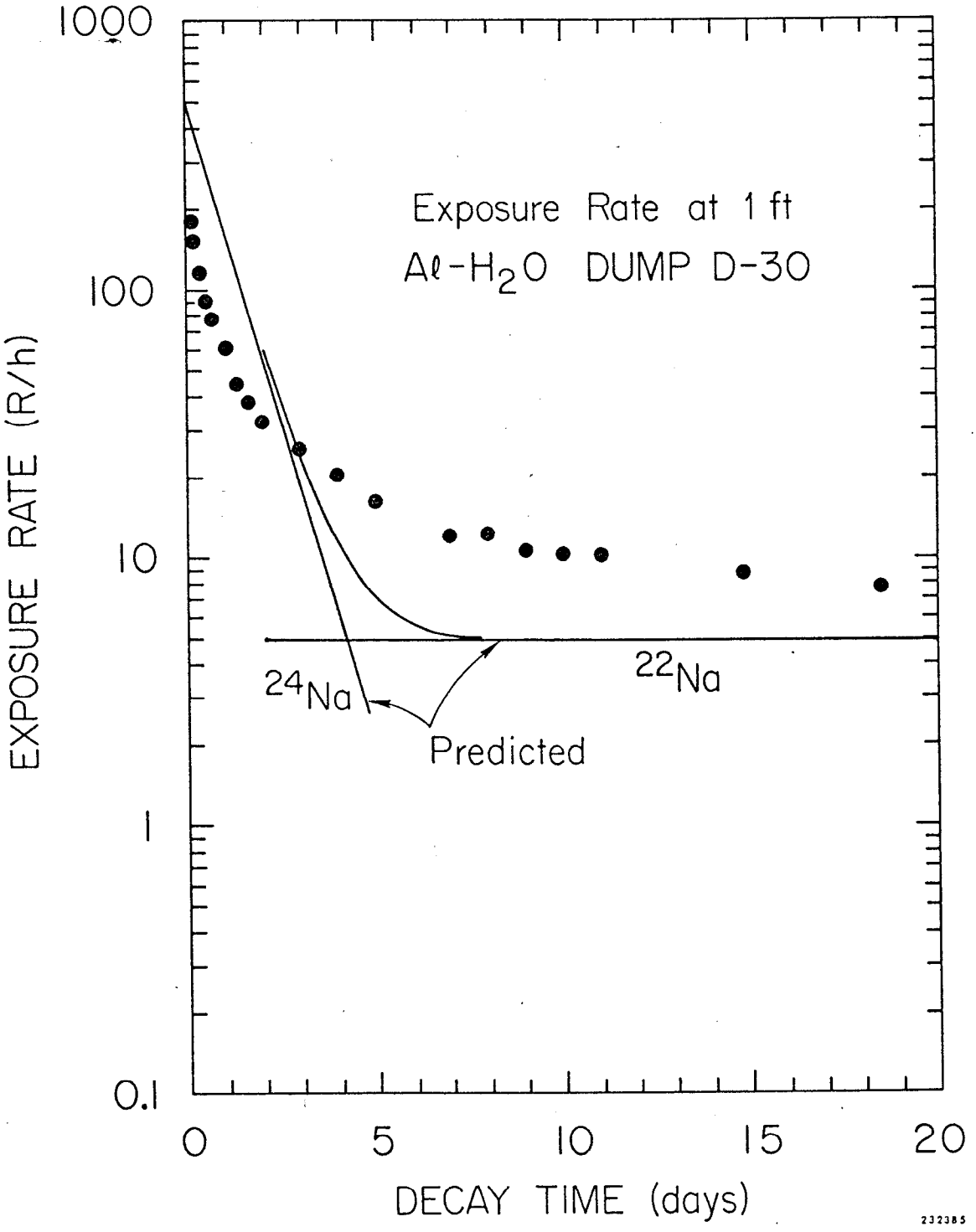
1000
100
10
1
0.1
EXPOSURE RATE (R/h)
Exposure Rate at 1 ft
Aℓ-H2O DUMP D-30
24Na
22Na
Predicted
0
5
10
15
20
DECAY TIME (days)
232385

Fig. 6